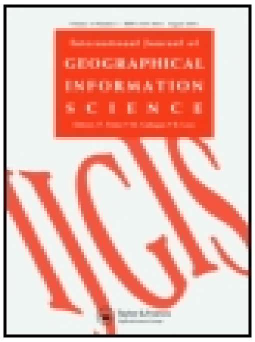

Taylor & Francis
Taylor & Francis Group

International Journal of Geographical Information Science

ISSN: 1365-8816 (Print) 1362-3087 (Online) Journal homepage: http://www.tandfonline.com/loi/tgis20

Mining transition rules of cellular automata for simulating urban expansion by using the deep learning techniques

Jialv He, Xia Li, Yao Yao, Ye Hong & Zhang Jinbao

To cite this article: Jialv He, Xia Li, Yao Yao, Ye Hong & Zhang Jinbao (2018): Mining transition rules of cellular automata for simulating urban expansion by using the deep learning techniques, International Journal of Geographical Information Science, DOI: 10.1080/13658816.2018.1480783

To link to this article: https://doi.org/10.1080/13658816.2018.1480783

Published online: 06 Jun 2018.

INTERNATIONAL JOURNAL OF GEOGRAPHICAL INFORMATION SCIENCE
https://doi.org/10.1080/13658816.2018.1480783

RESEARCH ARTICLE

Mining transition rules of cellular automata for simulating urban expansion by using the deep learning techniques

Jialv He [b], Xia Li [a,b], Yao Yao [c,d], Ye Hong [e] and Zhang Jinbao [b]

[a]School of Geographic Sciences, Key Lab. of Geographic Information Science (Ministry of Education), East China Normal University, Shanghai, P.R. China; [b]School of Geography and Planning, Guangdong Key Laboratory for Urbanization and Geo-simulation, Sun Yat-sen University, Guangzhou, China; [c]School of Information Engineering, China University of Geosciences, Wuhan, China; [d]Department of Data Technology and Products, Alibaba Group, Hangzhou, China; [e]Department of Civil, Environmental and Geomatic Engineering, ETH Zurich, Zürich, Switzerland

ABSTRACT

Along with the gradually accelerated urbanization process, simulating and predicting the future pattern of the city is of great importance to the prediction and prevention of some environmental, economic and urban issues. Previous studies have generally integrated traditional machine learning with cellular automaton (CA) models to simulate urban development. Nevertheless, difficulties still exist in the process of obtaining more accurate results with CA models; such difficulties are mainly due to the insufficient consideration of neighborhood effects during urban transition rule mining. In this paper, we used an effective deep learning method, named convolution neural network for united mining (UMCNN), to solve the problem. UMCNN has substantial potential to get neighborhood information from its receptive field. Thus, a novel CA model coupled with UMCNN and Markov chain was designed to improve the performance of simulating urban expansion processes. Choosing the Pearl River Delta of China as the study area, we excavate the driving factors and the transformational relations revealed by the urban land-use patterns in 2000, 2005 and 2010 and further simulate the urban expansion status in 2020 and 2030. Additionally, three traditional machine-learning-based CA models (LR, ANN and RFA) are built to attest the practicality of the proposed model. In the comparison, the proposed method reaches the highest simulation accuracy and landscape index similarity. The predicted urban expansion results reveal that the economy will continue to be the primary factor in the study area from 2010 to 2030. The proposed model can serve as guidance in urban planning and government decision-making.

ARTICLE HISTORY
Received 3 June 2017
Accepted 18 May 2018

KEYWORDS
Urban expansion; cellular automata; large scale; deep learning; Markov chain

1. Introduction

In the past few decades, the rapid development of urbanization has become a high-profile phenomenon in society (Wang *et al*. 2013a, Feng *et al*. 2016). Along with the development of human society, the increment in non-agricultural population and the conversion of urban development, urban scale is incessantly expanding at present (Glaeser and Kahn 2004, Helbich and Leitner 2010). The growth of cities promotes the

CONTACT Xia Li lixia@geo.ecnu.edu.cn; Yao Yao yaoy@cug.edu.cn

progress of human society and boosts the development of national economies. Nevertheless, quite a few cities are progressing at an excessive speed, which results in numerous urban problems, such as suburban environmental pollution and chaotic public order (Seto *et al*. 2012, Wang *et al*. 2013b). To alleviate these contradictions and maintain the human–land coordination and the sustainable development of society, decision makers should make exact judgments on the extent of urban expansion, thus setting urban development boundaries (Weng 2001, Jiang and Yao 2010). Consequently, the simulation of urban expansion has drawn the attention of many urban planners and government officials. This study simulates and analyzes the expansion of a typical urban agglomeration in China.

Previous studies indicate that a cellular automaton (CA) model is able to effectively simulate complex geographical processes, especially in the study of spatial simulation during urban changes. Since the 1990s, CA models have been adopted by many pioneers around the world to simulate urban growth (Clarke *et al*. 1997, Clarke and Gaydos 1998, Wu and Webster 1998, Li and Yeh 2000, White and Engelen 2000). These studies revealed that we can simulate complex structures by defining several simple local rules, which provide a basis for relevant geographical analysis (Li and Yeh 2000). Quite a few spatial variables are required in simulating urban development using a CA model. In a particular model, each spatial variable corresponds to a parameter, which is inextricably linked with the presentation of the model. Clarke *et al*. (1997) decided to ascertain parameters with the naked eye, which was subjective and time consuming. Wu and Webster (1998) adopted logistic regression to obtain parameters, but difficulties occurred in tackling the intricate relationship between spatial variables. Clarke and Gaydos (1998) proposed a method that automatically calculates the difference between the simulation results and the actual situation using a computer, seeking the solution that leads to the minimum error. Although the accuracy of this method was high and unconstrained by the complexity of the model, it was fairly inefficient. With the development of computer technology, machine-learning algorithms gradually entered this research field. Algorithms such as Artificial Neural Network (ANN) (Li and Yeh 2002, Basse *et al*. 2014), Random Forests Algorithm (RFA) (Biau 2012, Kamusoko and Gamba 2015), Genetic Algorithm (GA) (Li *et al*. 2013) and Support Vector Machine (SVM) (Yang *et al*. 2008) have been employed to cope with the parameter optimization issue of CA models. These methods can optimize the model's parameters and obtain the best result efficiently, which solves the complex geo-simulation problems associated with multiple spatial variables.

Although the traditional machine learning algorithm has optimized the geo-simulation model, it is still difficult to achieve high simulation accuracy (Lin and Li 2015). In addition to the subjective factors such as the instability of data quality and the rationality and randomness of neighborhood selection, the algorithm module of urban development suitability also requires improving. Generally, there are some traditional algorithms such as logistic regression, ANN and RFA. ANN is superior to logistic regression when we need to handle the complex relationships between spatial variable. RFA has the ability to obtain the better result than ANN. However, they merely accounted for a single pixel in mining the urban development suitability evaluated according to location factors and site properties (Li and Yeh 2000). To consider the neighborhood information when we calculate the urban development suitability, we used the deep learning techniques. Deep learning, which possesses strong learning ability, attains good effects in image processing and mining deep semantic features in text analysis. As a typical deep learning algorithm, the Convolutional Neural Network (CNN) uses the convolution kernel to extract the image information, taking full consideration of the neighborhood information of each pixel in the image (LeCun *et al*. 2015). Jean *et al*. (2016) adopts CNN to extract high-level semantic information in satellite imagery, thereby obtaining the distribution of impoverished areas in Africa. Zhong *et al*. (2016) used the improved large patch Convolutional Neural Network to classify the high-resolution image set. Based on the Convolution Neural Network for United Mining (UMCNN), Yao *et al*. (2018) combined high-resolution images and high-level semantic features of the driving force factor data to estimate the real estate price distribution in Shenzhen, China. Therefore, how to introduce deep learning into the process of geographical simulation and whether joint mining will enhance the accuracy of traditional geographical simulation have become very interesting questions.

To verify the effectiveness of the deep learning techniques in urban simulation, we use the urban development suitability calculated by deep learning techniques to construct the CA model. CA is a bottom-up approach in modeling complex systems, such as geographical process modeling and urban expansion simulation (Li and Yeh 2002, Yao *et al*. 2017a). The prediction ability of the CA model is illustrated by adopting Markov chain to calculate the total area of urban in the future. Markov chain has a key-descriptive tool, which is the transition probability matrix. An integration of CA and Markov chain has been already demonstrated to be an efficient hybrid geospatially explicit approach (Arsanjani *et al*. 2013).

In short, the purpose of this study is to combine deep learning, Markov chain and CA models. First, based on the conducted UMCNN training network, we obtained the overall development probability of the city by sampling and training the factors relating to urban dynamics in the study area. Second, by inputting the future urban growth amount predicted by the Markov chain, the simulation results of the CA model were attained. To verify the practicability of the model, several control groups using the traditional CA model are constructed to simultaneously compare the simulation accuracy and landscape similarity.

2. Study area and data

The study area of this research is the Pearl River Delta, which covers a total area of 54,219.98 km^2. It is an important economic zone in China (Yao *et al*. 2017b), with administrative areas including Guangzhou, Shenzhen, Zhuhai, Dongguan, Zhongshan, Jiangmen, Foshan, Huizhou and Zhaoqing, as shown in Figure 1.

The Pearl River Delta region has been experiencing rapid urbanization since the implementation of reform and opening-up policy in 1978 (Yeh and Li 1999, Lin and Li 2015). In this area, although fragmented and dotted construction areas occur in numerous small towns, there is a connecting tendency on the whole (Liu *et al*. 2017). The Pearl River Delta region involves a particular integrated development of urban and rural areas, in which cities develop along a high-quality transport network. With this rapid urban development, land use in the Pearl River Delta region is of great complexity and has thus led to a series of environmental, economic and urban development issues (Haas and Ban 2014).

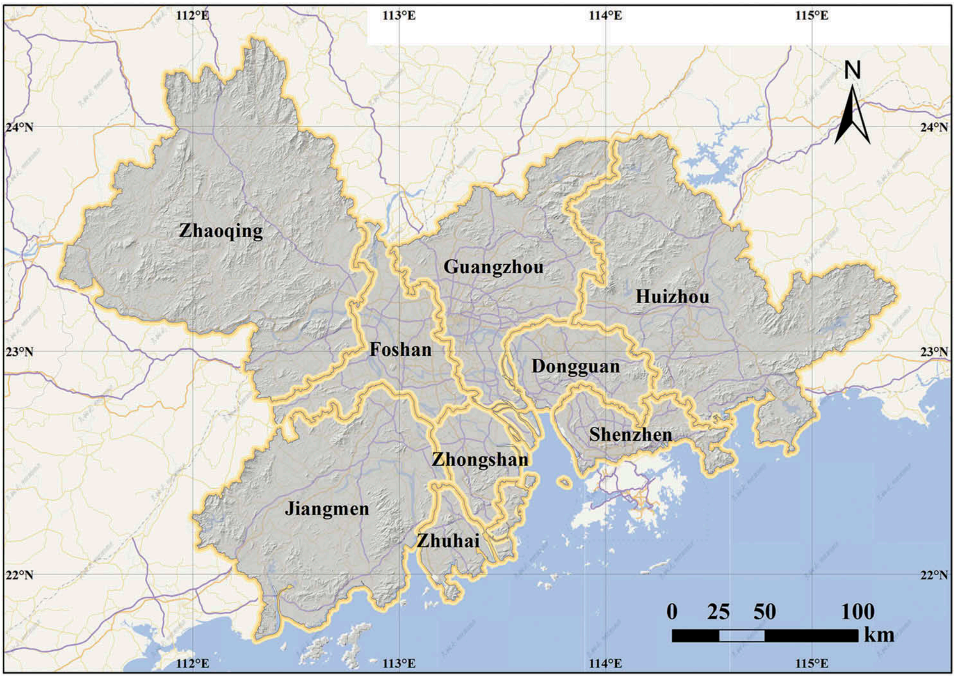

Figure 1. Location of the Pearl River Delta.

With the rapid development of modern cities, forecasting the development trends and planning the urban morphology of the cities in the Pearl River Delta is of great importance in transportation safety and urban construction (Weng 2002, Fu *et al*. 2003, Chen *et al*. 2011, Haas and Ban 2014). To construct a multi-period CA model, this study adopts the urban land use in 2000, 2005 and 2010, as shown in Figure 2. The spatial resolution of our land cover classification is 100 m with 4220 columns and 3221 rows. Specifically, urban land use occupies 7.98% of the total area in 2000, 11.94% in 2005 and 14.98% in 2010, generating an expansion of 7.09% over this decade.

Using the statistics for urban and non-urban land in various cities of the Pearl River Delta, each city's urban land-use proportion and expansion rate for the three years are calculated and shown in Table 1. More specifically, a1 indicates the urban expansion rate from 2000 to

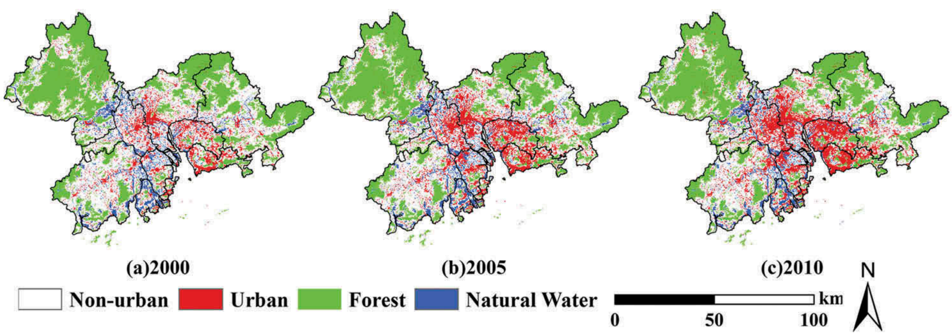

Figure 2. Land-use data of the Pearl River Delta for the simulation of urban expansion.

Table 1. Urban land use proportion in cities inside the Pearl River Delta. a_1: expansion ratio from 2000 to 2005, a_2: expansion ratio from 2005 to 2010, a_3: expansion ratio from 2000 to 2010. Pearl River Delta (PRD), Guangzhou (GZ), Foshan (FS), Shenzhen (SZ), Dongguan (DG), Huizhou (HZ), Jiangmen (JM), Zhaoqing (ZQ), Zhuhai (ZH), Zhongshan (ZS).

	2000	2005	2010	a_1	a_2	a_3
PRD	7.89%	11.94%	14.99%	4.05%	3.05%	7.10%
GZ	11.56%	17.55%	21.96%	5.99%	4.41%	10.40%
FS	14.73%	25.01%	31.98%	10.28%	6.97%	17.25%
SZ	30.78%	40.56%	50.67%	9.78%	10.11%	19.89%
DG	26.30%	45.99%	56.29%	19.70%	10.30%	29.99%
HZ	3.73%	5.44%	7.14%	1.71%	1.70%	3.41%
JM	5.85%	7.17%	9.29%	1.32%	2.12%	3.44%
ZQ	1.90%	2.63%	3.17%	0.72%	0.55%	1.27%
ZH	14.68%	19.94%	24.31%	5.26%	4.37%	9.63%
ZS	12.36%	24.95%	30.68%	12.59%	5.73%	18.32%

2005, a2 represents the urban expansion rate from 2005 to 2010, while a3 indicates the total urban expansion ratio of this decade. As the table shows, the largest city expansion ratio during this period was generated in Dongguan City, where urban land use increased by 29.99%, while the urban areas of Foshan City, Zhongshan City and Shenzhen City increased by 17.25%, 18.32% and 19.89%, respectively, which was consistent with Chinese policies over the years. In contrast, the development of Zhaoqing City, Jiangmen City and Huizhou City were slow, where urban land use merely increased by 1.27%, 3.41% and 3.44%, respectively. Owing to geographical disadvantage or policy drift, the development speed of these cities was far lower than other regions in this decade (Lin and Li 2015).

For large-scale land-use change simulation, complete land-use change driving factor data should be collected to obtain better simulation results for the entire study area. This paper accounts for the driving factors of urban development from the aspects of transportation, topography, government decision and water area (Liu *et al.* 2017). Moreover, we obtained the driving factors shown in Figure 3. The original data are normalized to [0,1].

3. Methodology

Our proposed method is integrated by UMCNN, CA model and Markov chain. We adopt UMCNN to calculate the urban development suitability, which acts as an input parameter of the CA model to simulate the future urban development of the Pearl River Delta region. Figure 4 shows the flowchart of this study. The study is divided into the following steps. (1) Based on the existing urban land-use data and auxiliary data in the Pearl River Delta, we constructed the driving factor data set and the sampled the land-use change data. (2) With the sample data and driving factor data set, the UMCNN model is trained and the optimal deep learning model is selected based on the accuracy of network training. Then, the softmax trainer in the UMCNN model is removed, and the remaining high-dimensional vector data set is extracted, which acts as an input in the RFA model to obtain the urban development suitability. (3) The overall urban development probability, calculated by the urban development suitability, neighborhood effects, constraint factors and stochastic factors, is used to simulate the data of the known year, which rectified the input parameters of the CA model. (4) By using the Markov chain, the urban growth amount in the future is predicted as the total prediction

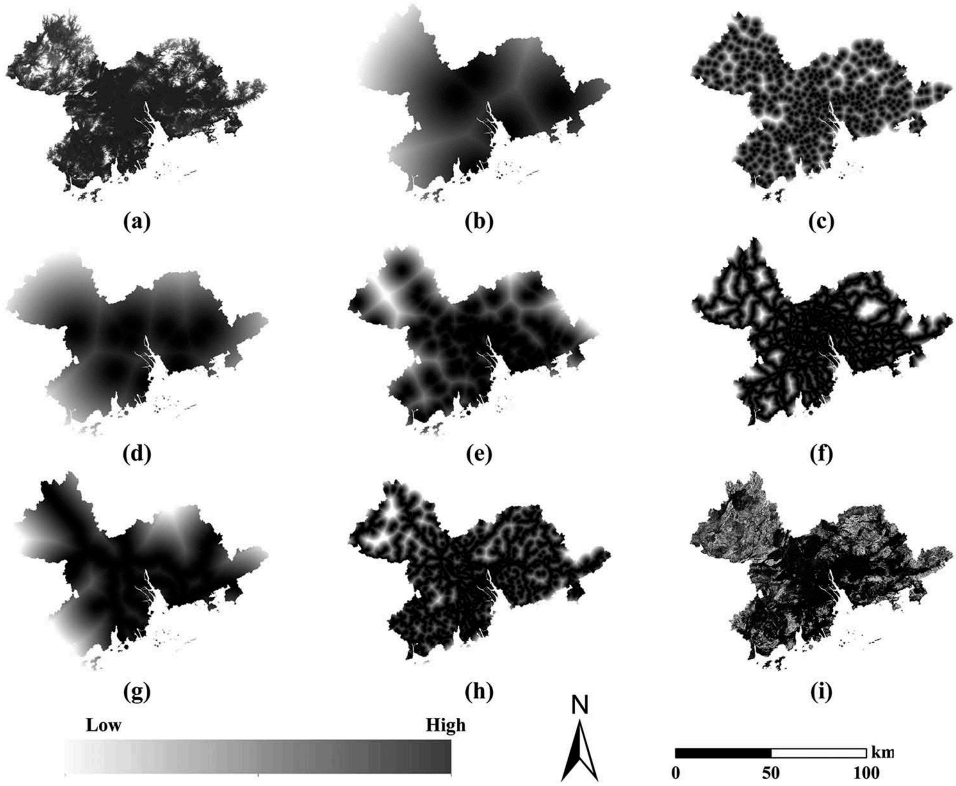

Figure 3. The driving factors in the Pearl River Delta. (a) DEM, (b) distance to airports, (c) distance to town centers, (d) distance to railway stations, (e) distance to trunk roads, (f) distance to highways, (g) distance to railways, (h) distance to rivers, (i) slope.

area, and is regarded as input data in the CA model to obtain urban development in the future. We input the maximum iteration times additionally to avoid the loop time of CA is considerably large. To attest the accuracy and practicability of the proposed model, the logistic regression CA model (Arsanjani *et al.* 2013), artificial neural network CA model (ANN-CA) (Li and Yeh 2002) and the random forest CA model (RFA-CA) (Kamusoko and Gamba 2015) are constructed to serve as contrast experiments.

3.1 *Setting and training of UMCNN*

As shown in Figure 5, the UMCNN model of this study includes seven layers, including three convolution layers, two max-pooling layers, one fully connected layer and one softmax layer (Krizhevsky *et al.* 2012, Yao *et al.* 2018). The activation function adopted in the convolution layers and the full-connection layer is the Rectified Linear Units (RELU), which can improve the training speed without losing the network accuracy and can reduce the probability of gradient disappearance (Krizhevsky *et al.* 2012). Previous studies also indicate that the use of small data sets could effectively reduce the complexity of the CNN network to avoid the emergence of over-fitting problems (Zhong *et al.* 2016). Hence, this study adds dropout operation in the convolution layers and the

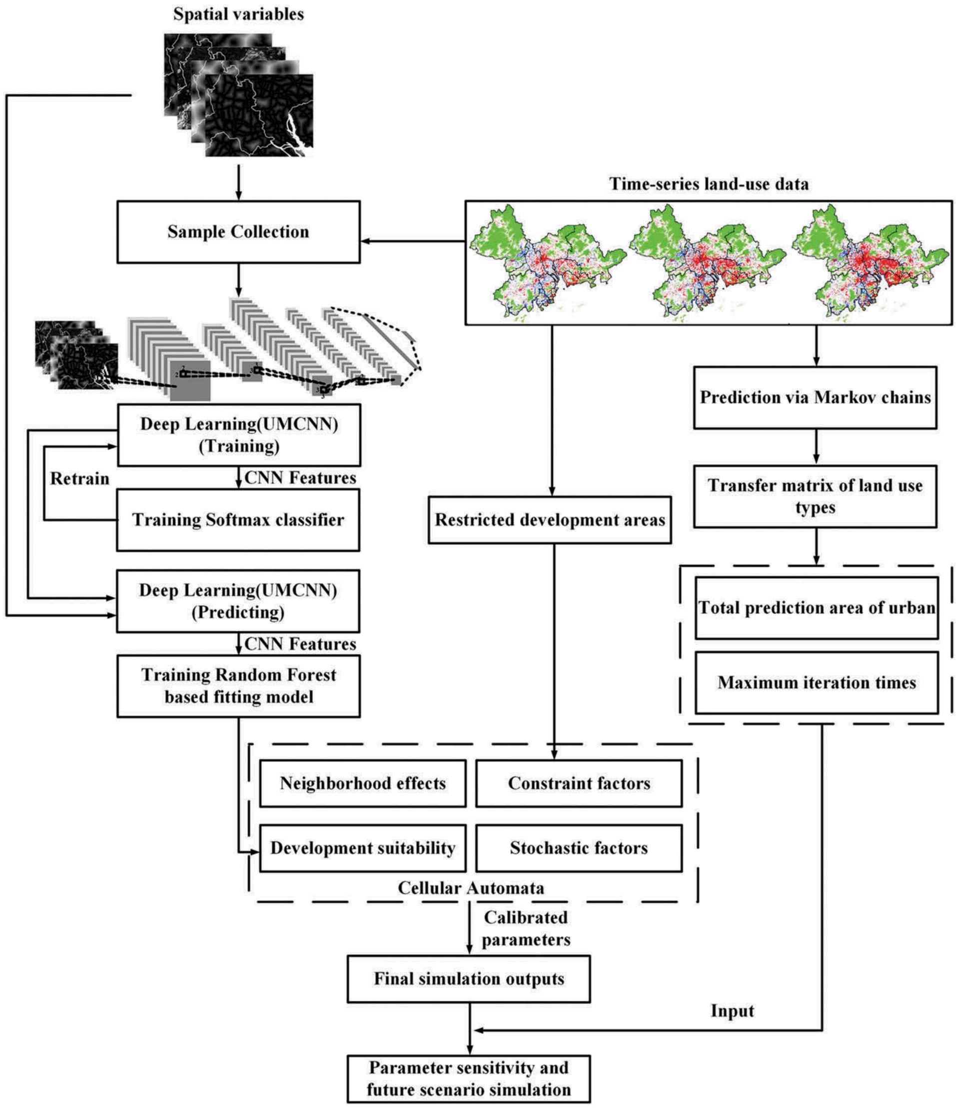

Figure 4. The flowchart of simulating urban expansion via UMCNN-CA.

full-connection layer, which prevents the case of over-fitting by randomly discarding the weight in the network (Hinton *et al.* 2012).

In this study, the UMCNN model adopts a 3 × 3 convolution kernel and a 2 × 2 pooling layer (Simonyan and Zisserman 2014). As mentioned above, the model adopts nine driving factor layers altogether, where patch size of the initial input data is 50 × 50. According to Figure 5, the first layer is the convolution layer. As the first layer consists of sixteen 3 × 3 convolution kernels, a feature image of 48 × 48 × 16 is exported after inputting the initial data. The second layer is composed of a pooling layer of 2 × 2, eventuating a feature image of 48 × 48 × 16. As the third layer establishes thirty-two convolution kernels of 3 × 3, input data will be converted to 22 × 22 × 32. The fourth layer is also a pooling layer of 2 × 2, where a dimensional feature image of 11 × 11 × 32

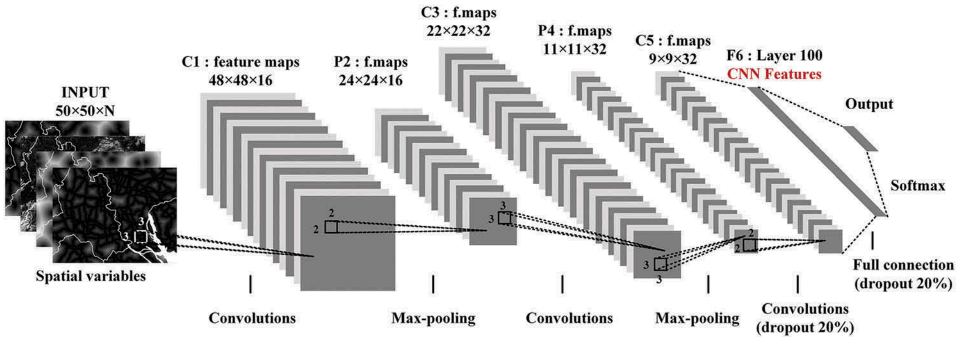

Figure 5. The computation framework of proposed UMCNN.

is obtained after pooling the input data. Similar to the convolution kernel of the third layer, the fifth layer turns the feature image into 9 × 9 × 32 (Yao *et al*. 2018). This is followed by the full-connection layer of the sixth layer, where 100 neurons are adopted. Finally, the classification result is obtained using softmax regression. Figure 6 shows an example of the working process of the sampling windows. The receptive field of UMCNN is the convolution kernel, which is used to extract feature from multiple spatial variables and calculate development suitability. By adopting the convolution kernel, more information can be considered compared to traditional methods (Schmidhuber 2015). To avoid over-fitting, dropout layers that randomly discard 20% of the network are added in front of the fifth and sixth layers. In particular, after training the UMCNN model, the

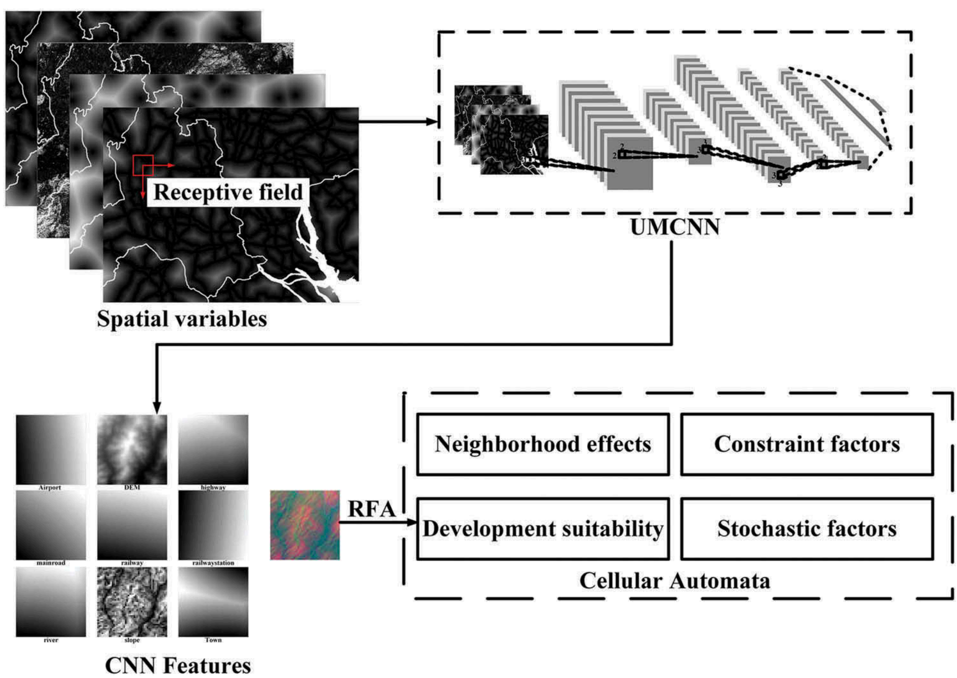

Figure 6. The working process of convolutional neural network.

softmax regression layer is removed and the RFA classifier only incorporates high-dimensional features of the upper layer to obtain the ultimate urban development suitability. Previous studies have verified that RFA classifier is the state-of-the-art machine learning models, which is able to obtain the better classification and fitting results than other machine learning classifiers and regression methods (Biau 2012, Fernández-Delgado *et al*. 2014). RFA is an aggregation of the Decision Tree. By using the bagging method, a new sub-dataset is generated by extracting random samples from the original training dataset (Breiman 2001, Biau 2012). When each decision tree selects random feature, it is constructed from each training sub-dataset, and they are not pruned during the growth process. We can obtain an Out-Of-Bag (OOB) from the estimation error report for each decision tree. The generalization error of RFA can be obtained by calculating the mean value of the errors of the decision trees. RFA has ability to solve the correlative problems among multiple spatial variables, especially in high-dimensional fitting situations (Palczewska *et al*. 2014).

3.2 *UMCNN-based cellular automata (UMCNN-CA)*

Proximity is one of the essential geospatial elements that emphasize the dynamics of various change events (Arsanjani *et al*. 2013). Previous studies have shown that neighborhood configuration affects the effects and the role of the CA model (Li *et al*. 2017). The transformation probability P of each cell in the traditional CA model is composed of four parts: overall development suitability *Pg*, neighborhood effectΩ, constraint coefficient *Pc* and stochastic factor *RA*.

The calculation of overall development suitability *Pg* in the CA model is mostly based on socioeconomic, geographical and ecological factors. In general, some statistical models, such as logistic regression, are used. However, how to determine the weight of different driving factors is so complex that it cannot be expressed with simple mathematical models, so machine learning models such as artificial neural networks are adopted. Compared with the artificial neural network, the deep learning network used in this paper is more suitable for mining the driving factors in large scale and large data volume, to obtain more exact overall development suitability *Pg*.

Next, neighborhood effect Ω is a vital characteristic factor in the CA model, which can effectively prevent broken and messy layout in the expansion simulation (Li and Yeh 2002, Dahal and Chow 2015). The most frequently employed neighborhoods are the von Neumann neighborhood, Moore neighborhood and the extended square neighborhood. The selection of neighborhoods in the CA model is very likely to produce disparate effects, so the choice of neighborhood has always been a very critical and complex problem in CA simulation (Li *et al*. 2017).

Constraint coefficient *Pc* is a specific land-use category that is not permitted to convert into urban land during the simulation process (Liu *et al*. 2012, Lin and Li 2016). In this study, water areas are deemed a constraint type, that is, water areas cannot develop into cities. Moreover, urban land-use change is of great complexity and randomness (Li and Yeh 2002, Wu and Martin 2002). To append stochastic factors into the CA model, this study introduced stochastic factor *RA*. In short, the probability that a single cell will convert at time t is described as follows:

$$P_{i,k}^t = Pg_{i,k}^t \cdot \Omega_i^t \cdot Pc_i^t \cdot RA$$

where $P_{i,k}^t$ is the probability that cell i converts to the k-state at time t. As for the actual situation in this study, $P_{i,k}^t$ also represents the total development probability of non-urban land converted to urban land at time t. $Pg_{i,k}^t$ is the overall development suitability of cell i at time t. Ω_i^t refers to the neighborhood effect of cell i at time t. Pc_i^t represents the constraint factors of the cell's development. *RA* is a random factor, which shifts in the range of 0–1. During the simulation, we compute the $Pg_{i,k}^t$ by UMCNN. The constraint factor is water and the neighborhood we chose is the von Neumann neighborhood. Then, we input the $P_{i,k}^t$ into the CA model to simulate urban expansion.

This study uses a Markov chain to predict future urban growth amount. A Markov chain is a stochastic process model that can be used to describe the transition process from one state to another within a system (Green 1995). To simulate the urban development status of 2020 and 2030 in the future, the Markov chain model uses multi-period land-use data, thus obtaining the transition matrix of state change at the corresponding time (Arsanjani *et al*. 2013, Guan *et al*. 2011, Yang *et al*. 2012, 2014).

3.3 *Accuracy assessment and uncertainty analysis*

To test and evaluate the urban expansion result simulated by the above-mentioned model, this study is evaluated from two aspects: cell and landscape pattern. At the cell level, previous studies have mostly adopted the overall accuracy (OA) and Kappa coefficient to verify accuracy (Arsanjani *et al*. 2013, Li *et al*. 2008, Liu *et al*. 2008). Nevertheless, many studies believe that the confusion matrix is unqualified to evaluate the accuracy of geographical simulation, especially under large-scale data volume. Unlike the classic methods, Pontius et al. proposed the use of Figure of Merit (FoM) to evaluate the model's accuracy, which is primarily determined by the numbers of variations in the simulation process (Pontius *et al*. 2007).

$$FoM = B/(A + B + C + D)$$

$$Product's\ accuracy\,(PA) = B/(A + B + C)$$

$$User's\ accuracy\,(UA) = B/(B + C + D)$$

where A is the area of error due to observed change predicted as persistence, B is the area of correctness due to observed change predicted as change, C is the area of error due to observed change predicted as change to the wrong category (here C should be set as 0 because the UMCNN-CA only simulates the change of non-urban cells), and D is the area of error due to observed persistence predicted as change (Chen *et al*. 2016, Yao *et al*. 2017a).

From the perspective of landscape pattern, we use a series of landscape pattern indices: the number of urban patches (NP), mean Euclidean nearest-neighbor distance (ENN) and mean perimeter-area ratio (PARA), which could all be calculated with FRAGSTATS 4.2 (McGarigal *et al*. 2012). The pattern-level similarity is measured based on the above indicators, which can distinguish the differences between the predicted image and the actual image (Chen *et al*. 2013, 2016).

$$a_l = 1 - \frac{1}{n}\sum_{i}^{n} \Delta l_i$$

$$\Delta l_i = \frac{\left| l_{i,s} - l_{i,o} \right|}{l_{i,o}} \times 100\%, l = NP, ENN, PARA$$

where $l_{i,s}$ and $l_{i,o}$ represent the landscape indices of the i-th prediction and the actual image, respectively, and Δl_i is the normalized result of all the indices. a_l is the similarity of the landscape pattern, calculated by means of Δl_i. n is the number of landscape indices, set as 3 in this study since three types of landscape indices are used.

4. Results

4.1 *Implementation and results*

The UMCNN-CA model proposed in this study is established through known data from 2000, 2005 and 2010. Moreover, to verify the utility of this model, the model's simulation accuracy is compared to three other traditional CA models (RFA-CA (Kamusoko and Gamba 2015), ANN-CA (Li and Yeh 2002) and Logistic-CA (Arsanjani *et al*. 2013)). In the UMCNN module, the network's sampling window is set to 50 pixels. Then, 80% of the sample data is used as training data in the CNN model and the other 20% is employed as accuracy calculation and error feedback. Furthermore, after training the CNN module, the original softmax layer is replaced by RFA for the fitting process, where 60% of the data is adopted for training and the rest is used to assess the accuracy of the module.

This section uses known data from the years 2000, 2005 and 2010. First, using the data of the previous two years, model calibration and the urban simulation of 2005 are conducted simultaneously. Then, using the land-use status of the latter two periods, the urban simulation of 2005 is acquired using the calibrated model. Figures 7 and 8 demonstrate the actual and simulated urban land use results in 2005 and 2010 by using the four models mentioned above.

The accuracies are showed in Table 2. As shown in Table 2, in the simulated two years, UMCNN-CA can get good results with the highest overall accuracy, Kappa coefficient and FoM. Compared with the other three traditional models, the simulation result of UMCNN-CA increased by 5.60%–7.70% in 2005 and 10.00%–12.30% in 2010, which demonstrated that UMCNN-CA is more suitable in mining the transition rules. Previous studies also indicate that, compared to other machine-learning models, CNN possesses a stronger ability to automatically extract the characteristics and morphological features of the region, thus obtaining better pattern recognition results (Hinton *et al*. 2012, Krizhevsky *et al*. 2012).

In Table 3, the FoM of each city's simulation result in the Pearl River Delta region of 2010 is counted. In general, the FoM in the study area reached 0.346, which is significantly higher than the previous study (Chen *et al*. 2013, Lin and Li 2015). More specifically, Guangzhou, which is the capital of Guangdong Province, and Dongguan, Shenzhen, Zhongshan and Foshan, which are relatively developed, have above-average FoM. In contrast, the FoM values of Zhaoqing, Jiangmen, Huizhou and Zhuhai, which are relatively underdeveloped, are below 0.2, especially in Zhaoqing, with a city coverage rate of merely 3.17% in 2010, as shown in Table 1, which is far below the average level of the entire research areas. This

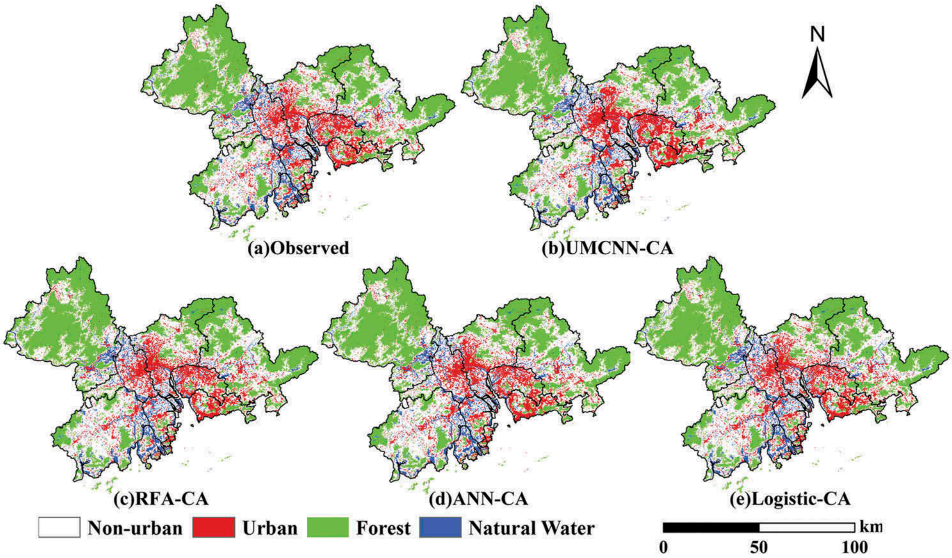

Figure 7. Simulated urban expansion by the four models for 2005.

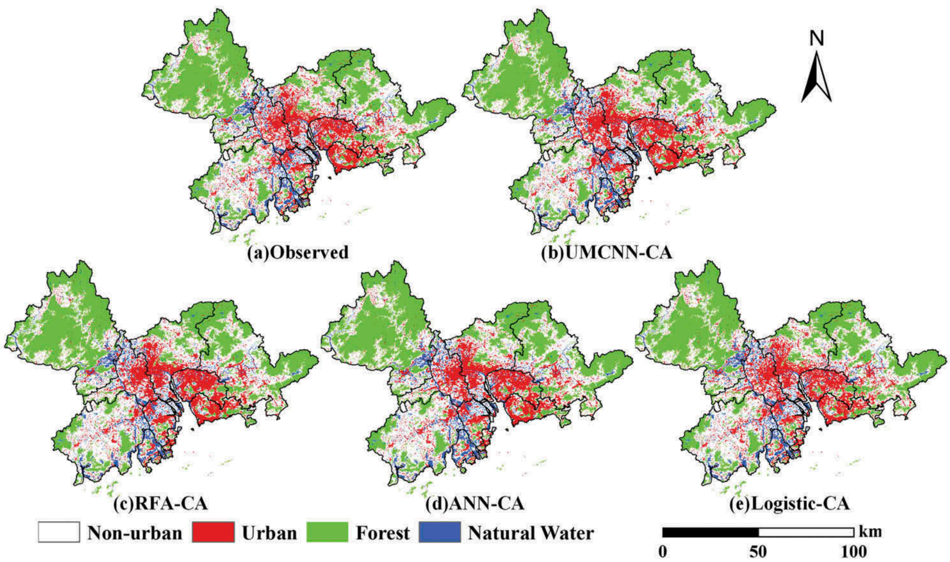

Figure 8. Simulated urban expansion by the four models for 2010.

result illustrates the complexity of urban development: Urban development in developed areas is mainly promoted by the conversion of interior urban land use. The development in economically backward areas is greatly dependent on the expansion of surrounding urban agglomerations, which is more susceptible to geographical factors, resulting in slow urban development (Dai *et al.* 2010, Wang *et al.* 2013b, Zheng *et al.* 2014).

We choose four typical areas from the simulated results in 2010 to illustrate the superiority of the proposed model as shown in Figure 9. On the one hand, obviously, the

Table 2. Comparison of the simulated results.

Simulation		UMCNN-CA	RFA-CA	ANN-CA	Logistic-CA
	OA	0.953	0.947	0.947	0.945
2005	Kappa	0.778	0.750	0.749	0.738
	FoM	0.268	0.212	0.210	0.191
	OA	0.931	0.924	0.924	0.923
2010	Kappa	0.729	0.703	0.703	0.701
	FoM	0.346	0.240	0.246	0.223

Table 3. FoM of the simulated results in different cities for 2010. Pearl River Delta (PRD), Guangzhou (GZ), Foshan (FS), Shenzhen (SZ), Dongguan (DG), Huizhou (HZ), Jiangmen (JM), Zhaoqing (ZQ), Zhuhai (ZH), Zhongshan (ZS).

	PA	UA	FoM
PRD	51.39%	51.39%	0.346
GZ	50.62%	53.86%	0.353
FS	48.52%	60.73%	0.369
SZ	59.11%	63.32%	0.440
DG	67.32%	70.17%	0.523
HZ	29.57%	35.45%	0.192
JM	35.61%	23.87%	0.167
ZQ	33.81%	12.47%	0.100
ZH	43.23%	24.12%	0.183
ZS	63.68%	51.84%	0.400

simulation generated by UMCNN-CA can better match the actual pattern than the results produced by other methods in the big cities such as Guangzhou and Shenzhen. On the other hand, it can also eliminate the phenomenon of ‘salt-and-pepper’. The UMCNN model, which fully accounts for the neighborhood information by using convolution kernels, is superior to other typical methods in the field of mining urban land-use transition rules and obtaining landscape pattern details.

Table 4 lists the comparative analysis of landscape indices for four different models at the landscape scale. As seen from the table, compared to the other three models, UMCNN-CA has a better performance in landscape similarity. In the simulation results for 2005, the landscape similarity between the UMCNN-CA simulation result and the actual result is 94.16%, with an NP value difference of merely 184, and the total similarity was 6.40%–7.86% higher than the other three models. Simulation results for 2010 declined slightly, but the proposed model still maintained a landscape similarity of 89.87% to 94.16%. In general, the above results reflected that UMCNN-CA obtains satisfactory effects in simulating the urban landscape.

4.2 *Parameters sensitivity analysis*

In the UMCNN-CA model, the size of the sampling window in UMCNN is not only closely related to the information mining in the original data but also plays a pivotal role in the simulation and accuracy of the subsequent CA model. Therefore, to explore the relationship between the size of the sampling window and the simulation accuracy, several verification tests are conducted. We conducted a set of experiments every 25 units from the window size of 25 × 25 to 150 × 150. Figure 10 shows the FoM from the simulation result for 2005 using truthful data from 2000 under different sampling windows. The simulation accuracy of

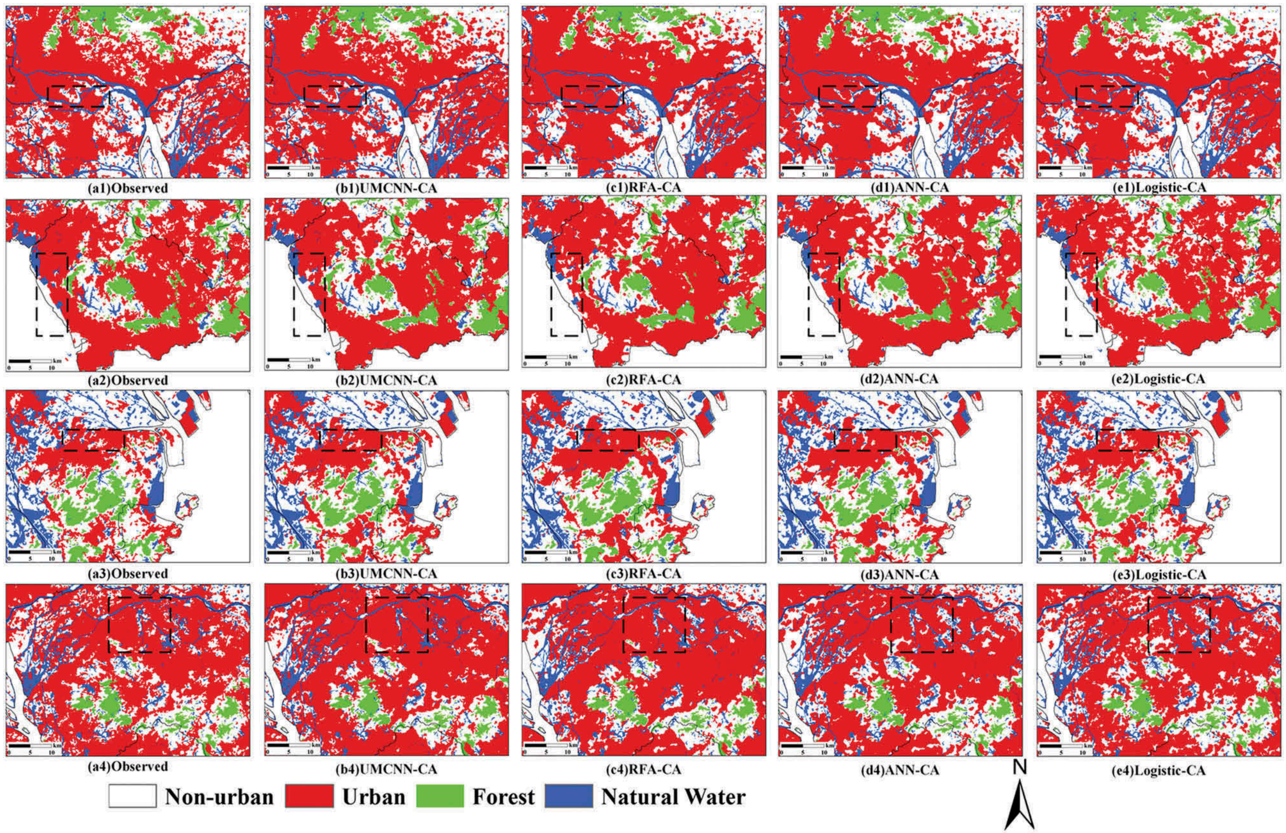

Figure 9. Comparison of simulated patterns for 2010 generated by several models (UMCNN-CA/RFA-CA/ANN-CA/Logistic-CA) in study area. (a1)–(e1) downtown areas of Guangzhou, (a2)–(e2) downtown areas of Shenzhen, (a3)–(e3) downtown areas of Zhongshan, (a4)–(e4) downtown areas of Dongguan.

Table 4. Comparison of observed and simulated values of landscape metrics. a_l: similarity of the landscape pattern.

	NP	PARA	ENN	a_l
2005				
Observed	7631	161.818	534.318	–
Simulated(UMCNN-CA)	7447	177.524	563.185	94.16%
Simulated(RFA-CA)	6062	161.137	618.434	87.76%
Simulated(ANN-CA)	6313	156.718	623.190	87.65%
Simulated(Logistic-CA)	6054	153.873	617.236	86.30%
2010				
Observed	7060	151.703	544.322	–
Simulated(UMCNN-CA)	6662	178.418	583.261	89.87%
Simulated(RFA-CA)	4842	151.150	658.483	82.42%
Simulated(ANN-CA)	4816	135.720	684.732	77.29%
Simulated(Logistic-CA)	5096	154.803	650.858	83.52%

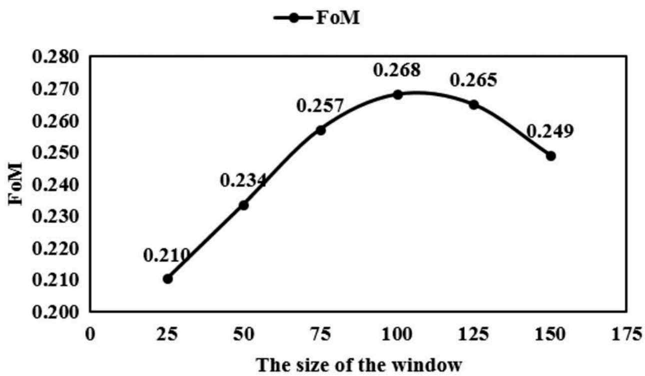

Figure 10. Accuracy assessment (y-axis) of UMCNN-CA in relation to the size of window (x-axis) for 2005.

UMCNN-CA varies between 0.210 and 0.268 with a significant trend, where the number gradually increases from 25 to 100 and begins to decline from 100.

Figure 11 shows the FoM results of employing different window sizes in the UMCNN-CA simulation for 2010. FoM alters from 0.321 to 0.346, although the span is much smaller than in 2005, yet with an evident trend. The simulation accuracy gradually

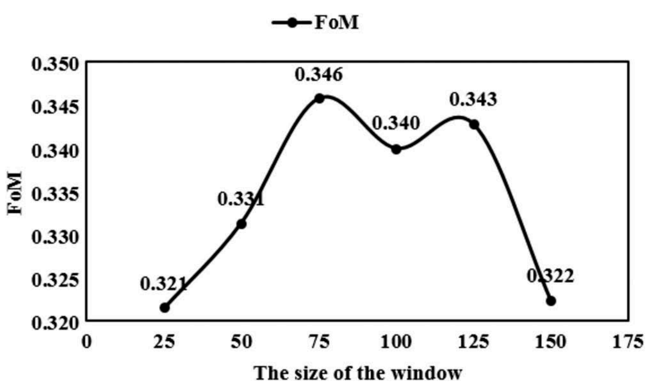

Figure 11. Accuracy assessment (y-axis) of UMCNN-CA in relation to the size of window (x-axis) for 2010.

increases with the sampling window size from 25 to 75 and peaks at 75. The accuracy is slightly lower between 75 and 100, but followed by a rising trend until 125, where the accuracy drops again. In general, this variation trend is similar to the one in the experiment for 2005, and the optimal sampling window size is in the range of 75–125. If the sampling window is set to be small, although the amount of computation is reduced, insufficient neighborhood information is under consideration. With a larger sampling window, however, excessive information may be mixed within a single window, affecting the accuracy of data mining (Zhong *et al*. 2016).

4.3 *Future scenarios simulation*

To forecast the future urban expansion in the Pearl River Delta, based on the Markov chain model and the combination of the urban and non-urban data for the known years, the transformational relation between the urban land and other lands is calculated and shown in Table 5. As shown in the table, the time span of the transfer matrix obtained by the model is limited to 10 years owing to the use of data for the two years of 2000 and 2010. As the total amount of land use in the study area remains the same, the land use of the next state can be predicted based on the 2010 data, which is the urban growth in 2020. Similarly, the urban growth of 2030 can be obtained based on the land-use data of 2020.

The total area of the study area is 54,219.98 km^2. As shown in Table 1, the urban area in 2010 is 8,127.58 km^2, and according to the conversion matrix in Table 5, the amount of urban growth is 2,172.36 km^2 in 2020 and is 3,407.14 km^2 in 2030. In the UMCNN-CA model, the future urban land use in these two years can be obtained by geographical simulation, taking the amount of urban growth of two future years, respectively, as shown in Figure 12.

Table 5. Markov transition probabilities matrix.

		Other	Urban			Other	Urban
Probability value of 2020 based on transition matrix of 2000–2010	Other	0.895	0.329	Probability value of 2030 based on transition matrix of 2000–2010	Other	0.835	0.515
	Urban	0.105	0.671		Urban	0.165	0.485

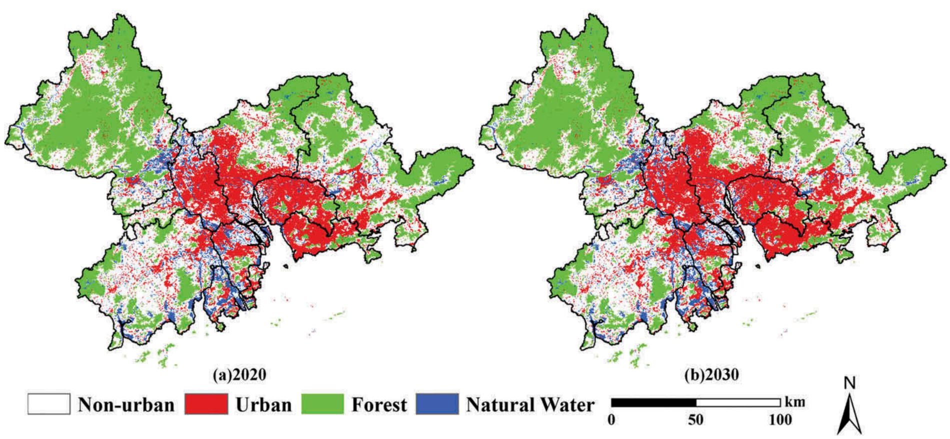

Figure 12. Simulations of urban expansion for the years 2020 and 2030.

Table 6. Expansion ratio of each city under future scenario simulation. a_1: expansion ratio from 2010 to 2020, a_2: expansion ratio from 2020 to 2030, a_3: expansion ratio from 2010 to 2030. Pearl River Delta (PRD), Guangzhou (GZ), Foshan (FS), Shenzhen (SZ), Dongguan (DG), Huizhou (HZ), Jiangmen (JM), Zhaoqing (ZQ), Zhuhai (ZH), Zhongshan (ZS).

	2010	2020	2030	a_1	a_2	a_3
PRD	14.99%	18.99%	21.27%	4.01%	2.28%	6.28%
GZ	21.96%	28.35%	31.75%	6.39%	3.39%	9.79%
FS	31.98%	45.27%	51.17%	13.29%	5.90%	19.19%
SZ	50.67%	60.91%	66.46%	10.24%	5.55%	15.79%
DG	56.29%	69.10%	72.72%	12.81%	3.62%	16.43%
HZ	7.14%	10.62%	13.19%	3.48%	2.56%	6.05%
JM	9.29%	10.92%	12.26%	1.63%	1.35%	2.97%
ZQ	3.17%	3.49%	3.87%	0.32%	0.38%	0.70%
ZH	24.31%	25.93%	27.98%	1.61%	2.05%	3.66%
ZS	30.68%	36.15%	40.49%	5.47%	4.34%	9.81%

Table 6 shows an overview of urban land-use growth in each city in the future scenario. a_1 represents the shifts in the proportion of urban land use from 2010 to 2020, a_2 indicates the changes from 2020 to 2030, and a_3 represents the total expansion rate over the 20 years. It can be seen from the table that: (1) In the next 20 years, the urban area in the Pearl River Delta region is expected to expand by 6.28%, with an 0.82% decrement in the expansion rate compared to the previous 10 years; (2) Dongguan, Foshan and Shenzhen are expected to maintain a relatively rapid pace of urban development; (3) Zhaoqing, Jiangmen and Huizhou are still developing at the slowest speed in the Pearl River Delta region.

Compared to the past decade, the future development areas in the Pearl River Delta are mainly encompassed by the developed economic region. Owing to abundant water bodies and forests, low urban density areas such as Zhaoqing and Jiangmen are not suitable for urban development. Thanks to the presence of urban agglomerations and affluent bare land and farmland, which retain great potential to develop into urban lands, high-density urban areas such as Shenzhen, Guangzhou, Foshan and Dongguan are expected to maintain a rapid pace of development (Haas and Ban 2014).

5. Discussion and conclusion

Urban expansion simulation has been a hot research topic, and how to accurately unearth the rules of urban land-use change has always been the key point of geographical simulation (Li *et al*. 2017). The purpose of this study is to verify the effectiveness of deep learning in urban simulation. To our knowledge, we are the first to integrate deep learning techniques with CA and Markov chain. To simulate urban expansion at a large scale, we selected the Pearl River Delta region as the research area and coupled the UMCNN, the Markov chain and the CA model. First, based on the driving factor data excavated by UMCNN model and the sample data of urban land-use change for known years, the urban development suitability of the whole study area was obtained by fitting the RFA model. Then, the CA model was constructed and further revised with the land-use simulation for 2005 and 2010. Last, by using the predicted urban growth amount in the next 10 and 20 years with the Markov chain as input parameter in the rectified CA model, the urban expansion state of the Pearl River Delta in 2020 and 2030 was simulated.

To verify the practicability of the proposed model, we constructed three traditional CA models, ANN-CA, RFA-CA and Logistic-CA (Arsanjani *et al*. 2013, Li and Yeh 2002, Kamusoko and Gamba 2015). As evidenced by comparing several experiments, the UMCNN-CA model obtains the best simulation accuracy (FoM_{2005} = 0.268, FoM_{2010} = 0.346), where the simulation result exceeds 5.60%–7.70% in 2005 and 10.00%–12.30% in 2010. In the aspect of landscape similarity, UMCNN-CA also got the highest similarity ($a_{l\text{-}2005}$ = 94.16%□$a_{l\text{-}2010}$ = 89.87%), where the results increased by 6.0%–7.66% in 2005 and 6.35%–12.58% in 2010. These results indicate that UMCNN can excavate the law of urban development more accurately under large-scale simulation, which is mainly due to the consideration of neighborhood influence and improvements in single-pixel calculation. Although the accuracy of the model is greatly affected by the size of the training window, its lowest simulation accuracy is still higher than the traditional CA model.

The process of urban development is fraught with uncertainty and complexity. Many studies regard the development of modern cities as a self-adaptive mechanism, which can be divided into a top-down pattern and a bottom-up pattern (Tian and Shen 2011, Long *et al*. 2012). Under this adaptive development cognition, urban land change is related not only to environmental factors but also to urban planning, government decision-making and human activities. These factors are of great complexity and randomness, which hinders the prediction of city simulation at the present stage. Therefore, although urban simulation using the UMCNN-CA model received better results compared with the traditional CA model, it is still inconsistent with the actual situation. In the future studies, we expect to take a more comprehensive account of the impact of the environment, socioeconomic and urban planning on urban development. Meanwhile, to construct a more stabilized UMCNN-CA model, mining conversion rules in different urban partitions, respectively, and adding more trainings in deep learning should be considered.

Chen *et al*. (2013) presented several possible scenarios in urban modeling (such as economic development and low-carbon urban). Based on these scenarios, more detailed city simulation and analysis can be executed in the future. Moreover, owing to the quality of the environmental driving factors in the CA model, accurate multi-period data is difficult to obtain. To solve this issue, Li *et al*. (2017) and Liu *et al*. (2017) proposed the FLUS-CA model, which uses merely a single period of driving factor data to forecast and simulate future land-use changes. In future work, we will also draw on the idea of the FLUS-CA model.

How to adjust the CNN parameters automatically, including the number of hidden layers and the size of the convolution kernel, has always been an open question in deep learning (Krizhevsky *et al*. 2012, Simonyan and Zisserman 2014, Abadi *et al*. 2016). Owing to the complexity of the UMCNN-CA model (Yao *et al*. 2018), adjusting the parameters manually will not only increase the overall run time of the model but also introduce subjective factors. Meanwhile, similar to traditional machine learning methods, it is difficult for the UMCNN model to measure the weight between various types of driving force factors. Hence, future work will attach importance to improving the parameter adjustment part and the overall efficiency of the model. In addition, other efficient deep learning techniques, such as autoencoder or deep belief network, might be able to be also considered as the tool to mine the transition rule of urban growth in future research.

In short, the proposed UMCNN-CA model achieves much higher simulation results than the traditional CA models, which is of great significance for future urban planning and government decision-making (Chen *et al*. 2016). With the acceleration of urbanization, it is increasingly difficult for the traditional model to meet the needs of contemporary urban simulation. The arrival of the information age has generated more vast and more diversified data with preferable quality. Accordingly, continuously improving the traditional CA model is of great significance for simulating and predicting future urban expansion. Future work will also emphasize diversified data, fine-scale urban expansion simulation and other aspects.

Acknowledgments

We would like to thank Prof. May Yuan, Prof. Bo Huang and three anonymous reviewers for their constructive suggestions that significantly strengthened this manuscript.

Funding

This study was supported by the Key National Natural Science Foundation of China (Grant No. 41531176).

Disclosure statement

No potential conflict of interest was reported by the authors.

Funding

This study was supported by the Key National Natural Science Foundation of China (Grant No. 41531176).

ORCID

Jialv He http://orcid.org/0000-0002-0997-558X
Xia Li http://orcid.org/0000-0003-3050-8529
Yao Yao http://orcid.org/0000-0002-2830-0377
Ye Hong http://orcid.org/0000-0002-8996-3748
Zhang Jinbao http://orcid.org/0000-0001-8510-149X

References

Abadi, M.I.N., *et al*., 2016. Tensorflow: large-scale machine learning on heterogeneous distributed systems. *arXiv preprint arXiv:1603.04467*.

Arsanjani, J.J., *et al*., 2013. Integration of logistic regression, Markov chain and cellular automata models to simulate urban expansion. *International Journal of Applied Earth Observation and Geoinformation*, 21, 265–275. doi:10.1016/j.jag.2011.12.014

Basse, R.M., *et al*., 2014. Land use changes modelling using advanced methods: cellular automata and artificial neural networks. The spatial and explicit representation of land cover dynamics at the cross-border region scale. *Applied Geography*, 53, 160–171. doi:10.1016/j.apgeog.2014.06.016

Biau, G.A.V.S., 2012. Analysis of a random forests model. *Journal of Machine Learning Research*, 13 (Apr), 1063–1095.

Breiman, L., 2001. Random forests. *Machine Learning*, 45 (1), 5–32. doi:10.1023/A:1010933404324

Chen, Y., *et al*. 2011. Estimating the relationship between urban forms and energy consumption: a case study in the Pearl River Delta, 2005–2008. *Landscape and Urban Planning*, 102 (1), 33–42. doi:10.1016/j.landurbplan.2011.03.007

Chen, Y., *et al*. 2013. Simulating urban form and energy consumption in the Pearl River Delta under different development strategies. *Annals of the Association of American Geographers*, 103 (6), 1567–1585. doi:10.1080/00045608.2012.740360

Chen, Y., *et al*., 2016. Capturing the varying effects of driving forces over time for the simulation of urban growth by using survival analysis and cellular automata. *Landscape and Urban Planning*, 152, 59–71. doi:10.1016/j.landurbplan.2016.03.011

Clarke, K.C. and Gaydos, L.J., 1998. Loose-coupling a cellular automaton model and GIS: long-term urban growth prediction for San Francisco and Washington/Baltimore. *International Journal of Geographical Information Science*, 12 (7), 699–714. doi:10.1080/136588198241617

Clarke, K.C., Hoppen, S., and Gaydos, L., 1997. A self-modifying cellular automaton model of historical urbanization in the San Francisco Bay area. *Environment and Planning B: Planning and Design*, 24 (2), 247–261. doi:10.1068/b240247

Dahal, K.R. and Chow, T.E., 2015. Characterization of neighborhood sensitivity of an irregular cellular automata model of urban growth. *International Journal of Geographical Information Science*, 29 (3), 475–497. doi:10.1080/13658816.2014.987779

Dai, X., *et al*. 2010. Spatio-temporal pattern of urban land cover evolvement with urban renewal and expansion in Shanghai based on mixed-pixel classification for remote sensing imagery. *International Journal of Remote Sensing*, 31 (23), 6095–6114. doi:10.1080/01431160903376407

Feng, Y., Liu, Y., and Batty, M., 2016. Modeling urban growth with GIS based cellular automata and least squares SVM rules: a case study in Qingpu–songjiang area of Shanghai, China. *Stochastic Environmental Research and Risk Assessment*, 30 (5), 1387–1400. doi:10.1007/s00477-015-1128-z

Fernández-Delgado, M., *et al*., 2014. Do we need hundreds of classifiers to solve real world classification problems. *Journal Mach Learning Researcher*, 15 (1), 3133–3181.

Fu, J., *et al*. 2003. Persistent organic pollutants in environment of the Pearl River Delta, China: an overview. *Chemosphere*, 52 (9), 1411–1422. doi:10.1016/S0045-6535(03)00477-6

Glaeser, E.L. and Kahn, M.E., 2004. Sprawl and urban growth. *In*: *Handbook of regional and urban economics*. Elsevier. 2481–2527.

Green, P.J., 1995. Reversible jump Markov chain Monte Carlo computation and Bayesian model determination. *Biometrika*, 82 (4), 711–732. doi:10.1093/biomet/82.4.711

Guan, D., *et al*., 2011. Modeling urban land use change by the integration of cellular automaton and Markov model. *Ecological Modelling*, 222(20–22), 3761–3772. doi:10.1016/j.ecolmodel.2011.09.009

Haas, J. and Ban, Y., 2014. Urban growth and environmental impacts in Jing-Jin-Ji, the Yangtze, River Delta and the Pearl River Delta. *International Journal of Applied Earth Observation and Geoinformation*, 30, 42–55. doi:10.1016/j.jag.2013.12.012

Helbich, M. and Leitner, M., 2010. Postsuburban spatial evolution of Vienna's urban fringe: evidence from point process modeling. *Urban Geography*, 31 (8), 1100–1117. doi:10.2747/0272-3638.31.8.1100

Hinton, G.E., *et al*., 2012. Improving neural networks by preventing co-adaptation of feature detectors. *arXiv preprint arXiv:1207.0580*.

Jean, N., *et al*. 2016. Combining satellite imagery and machine learning to predict poverty. *Science*, 353 (6301), 790–794. doi:10.1126/science.aaf7894

Jiang, B. and Yao, X., 2010. Geospatial analysis and modeling of urban structure and dynamics: an overview. *In*: *Geospatial analysis and modelling of urban structure and dynamics*. Dordrecht: Springer. 3–11.

Kamusoko, C. and Gamba, J., 2015. Simulating urban growth using a Random Forest-Cellular Automata (RF-CA) model. *ISPRS International Journal of Geo-Information*, 4 (2), 447–470. doi:10.3390/ijgi4020447

Krizhevsky, A., Sutskever, I., and Hinton, G.E., 2012. *Imagenet classification with deep convolutional neural networks*. Advances in neural information processing systems, Lake Tahoe, NV, 1097–1105.

LeCun, Y., Bengio, Y., and Hinton, G., 2015. Deep learning. *Nature*, 521 (7553), 436. doi:10.1038/nature14539

Li, X., *et al*. 2013. Calibrating cellular automata based on landscape metrics by using genetic algorithms. *International Journal of Geographical Information Science*, 27 (3), 594–613. doi:10.1080/13658816.2012.698391

Li, X., *et al*. 2017. A new global land-use and land-cover change product at a 1-km resolution for 2010 to 2100 based on human–environment interactions. *Annals of the American Association of Geographers*, 107 (5), 1040–1059. doi:10.1080/24694452.2017.1303357

Li, X., Yang, Q., and Liu, X., 2008. Discovering and evaluating urban signatures for simulating compact development using cellular automata. *Landscape and Urban Planning*, 86 (2), 177–186. doi:10.1016/j.landurbplan.2008.02.005

Li, X. and Yeh, A.G., 2000. Modelling sustainable urban development by the integration of constrained cellular automata and GIS. *International Journal of Geographical Information Science*, 14 (2), 131–152. doi:10.1080/136588100240886

Li, X. and Yeh, A.G., 2002. Neural-network-based cellular automata for simulating multiple land use changes using GIS. *International Journal of Geographical Information Science*, 16 (4), 323–343. doi:10.1080/13658810210137004

Lin, J. and Li, X., 2015. Simulating urban growth in a metropolitan area based on weighted urban flows by using web search engine. *International Journal of Geographical Information Science*, 29 (10), 1721–1736. doi:10.1080/13658816.2015.1034721

Lin, J. and Li, X., 2016. Conflict resolution in the zoning of eco-protected areas in fast-growing regions based on game theory. *Journal of Environmental Management*, 170, 177–185. doi:10.1016/j.jenvman.2015.11.036

Liu, X., *et al*. 2008. Simulating complex urban development using kernel-based non-linear cellular automata. *Ecological Modelling*, 211 (1–2), 169–181. doi:10.1016/j.ecolmodel.2007.08.024

Liu, X., *et al*. 2012. An integrated approach of remote sensing, GIS and swarm intelligence for zoning protected ecological areas. *Landscape Ecology*, 27 (3), 447–463. doi:10.1007/s10980-011-9684-1

Liu, X., *et al*., 2017. A future land use simulation model (FLUS) for simulating multiple land use scenarios by coupling human and natural effects. *Landscape and Urban Planning*, 168, 94–116. doi:10.1016/j.landurbplan.2017.09.019

Long, Y., Gu, Y., and Han, H., 2012. Spatiotemporal heterogeneity of urban planning implementation effectiveness: evidence from five urban master plans of Beijing. *Landscape and Urban Planning*, 108 (2–4), 103–111. doi:10.1016/j.landurbplan.2012.08.005

McGarigal, K., Cushman, S.A., and Ene, E., 2012. FRAGSTATS v4: spatial pattern analysis program for categorical and continuous maps. *In*: *Computer Software Program Produced by the Authors at the University of Massachusetts*, Amherst. Available from: http://www. umass. edu/landeco/research/fragstats/fragstats (Accessed 2 November 2016).

Palczewska, A., *et al*., 2014. Interpreting random forest classification models using a feature contribution method. *In*: *integration of Reusable Systems*. Berlin: Springer, 193–218.

Pontius, R.G., *et al*. 2007. Accuracy assessment for a simulation model of Amazonian deforestation. *Annals of the American Association of Geographers*, 97 (4), 677–695. doi:10.1111/j.1467-8306.2007.00577.x

Schmidhuber, J.U.R., 2015. Deep learning in neural networks: an overview. *Neural Networks*, 61, 85–117. doi:10.1016/j.neunet.2014.09.003

Seto, K.C., Neralp, G.U., and Hutyra, L.R., 2012. Global forecasts of urban expansion to 2030 and direct impacts on biodiversity and carbon pools. *Proceedings of the National Academy of Sciences*, 109 (40), 16083–16088. doi:10.1073/pnas.1211658109

Simonyan, K. and Zisserman, A., 2014. Very deep convolutional networks for large-scale image recognition. *arXiv preprint arXiv:1409.1556*.

Tian, L. and Shen, T., 2011. Evaluation of plan implementation in the transitional China: A case of Guangzhou city master plan. *Cities*, 28 (1), 11–27. doi:10.1016/j.cities.2010.07.002

Wang, H., *et al*., 2013a. Simulating urban expansion using a cloud-based cellular automata model: A case study of Jiangxia, Wuhan, China. *Landscape and Urban Planning*, 110, 99–112. doi:10.1016/j.landurbplan.2012.10.016

Wang, H., *et al*., 2013b. An integrated approach to supporting land-use decisions in site redevelopment for urban renewal in Hong Kong. *Habitat International*, 38, 70–80. doi:10.1016/j.habitatint.2012.09.006

Weng, Q., 2001. A remote sensing? GIS evaluation of urban expansion and its impact on surface temperature in the Zhujiang Delta, China. *International Journal of Remote Sensing*, 22 (10), 1999–2014.

Weng, Q., 2002. Land use change analysis in the Zhujiang Delta of China using satellite remote sensing, GIS and stochastic modelling. *Journal of Environmental Management*, 64 (3), 273–284. doi:10.1006/jema.2001.0509

White, R. and Engelen, G., 2000. High-resolution integrated modelling of the spatial dynamics of urban and regional systems. *Computers, Environment and Urban Systems*, 24 (5), 383–400. doi:10.1016/S0198-9715(00)00012-0

Wu, F. and Martin, D., 2002. Urban expansion simulation of Southeast England using population surface modelling and cellular automata. *Environment and Planning A*, 34 (10), 1855–1876. doi:10.1068/a3520

Wu, F. and Webster, C.J., 1998. Simulation of land development through the integration of cellular automata and multicriteria evaluation. *Environment and Planning B: Planning and Design*, 25 (1), 103–126. doi:10.1068/b250103

Yang, Q., Li, X., and Shi, X., 2008. Cellular automata for simulating land use changes based on support vector machines. *Computers & Geosciences*, 34 (6), 592–602. doi:10.1016/j.cageo.2007.08.003

Yang, X., Zheng, X., and Chen, R., 2014. A land use change model: integrating landscape pattern indexes and Markov-CA. *Ecological Modelling*, 283, 1–7. doi:10.1016/j.ecolmodel.2014.03.011

Yang, X., Zheng, X., and Lv, L., 2012. A spatiotemporal model of land use change based on ant colony optimization, Markov chain and cellular automata. *Ecological Modelling*, 233, 11–19. doi:10.1016/j.ecolmodel.2012.03.011

Yao, Y., *et al*. 2017a. Simulating urban land-use changes at a large scale by integrating dynamic land parcel subdivision and vector-based cellular automata. *International Journal of Geographical Information Science*, 31 (12), 2452–2479. doi:10.1080/13658816.2017.1360494

Yao, Y., *et al*. 2017b. Sensing spatial distribution of urban land use by integrating points-of-interest and Google Word2Vec model. *International Journal of Geographical Information Science*, 31 (4), 825–848. doi:10.1080/13658816.2016.1244608

Yao, Y., *et al*., 2018. Mapping fine-scale urban housing price by fusing remote-sensing image and social media data. *Transactions in GIS*. doi:10.1111/tgis.12330

Yeh, A.G. and Li, X., 1999. Economic development and agricultural land loss in the Pearl River Delta, China. *Habitat International*, 23 (3), 373–390. doi:10.1016/S0197-3975(99)00013-2

Zheng, H.W., Shen, G.Q., and Wang, H., 2014. A review of recent studies on sustainable urban renewal. *Habitat International*, 41, 272–279. doi:10.1016/j.habitatint.2013.08.006

Zhong, Y., Fei, F., and Zhang, L., 2016. Large patch convolutional neural networks for the scene classification of high spatial resolution imagery. *Journal of Applied Remote Sensing*, 10 (2), 25006. doi:10.1117/1.JRS.10.025006